



Deletion of the Akt/mTORC1 Repressor REDD1 Prevents Visual Dysfunction in a Rodent Model of Type 1 Diabetes

William P. Miller,¹ Chen Yang,¹ Maria L. Mihailescu,¹ Joshua A. Moore,¹ Weiwei Dai,¹ Alistair J. Barber,² and Michael D. Dennis¹

Diabetes 2018;67:110–119 | <https://doi.org/10.2337/db17-0728>

Diabetes-induced visual dysfunction is associated with significant neuroretinal cell death. The current study was designed to investigate the role of the Protein Regulated in Development and DNA Damage Response 1 (REDD1) in diabetes-induced retinal cell death and visual dysfunction. We recently demonstrated that REDD1 protein expression was elevated in response to hyperglycemia in the retina of diabetic rodents. REDD1 is an important regulator of Akt and mammalian target of rapamycin and as such plays a key role in neuronal function and survival. In R28 retinal cells in culture, hyperglycemic conditions enhanced REDD1 protein expression concomitant with caspase activation and cell death. By contrast, in REDD1-deficient R28 cells, neither hyperglycemic conditions nor the absence of insulin in culture medium were sufficient to promote cell death. In the retinas of streptozotocin-induced diabetic mice, retinal apoptosis was dramatically elevated compared with nondiabetic controls, whereas no difference was observed in diabetic and nondiabetic REDD1-deficient mice. Electroretinogram abnormalities observed in b-wave and oscillatory potentials of diabetic wild-type mice were also absent in REDD1-deficient mice. Moreover, diabetic wild-type mice exhibited functional deficiencies in visual acuity and contrast sensitivity, whereas diabetic REDD1-deficient mice had no visual dysfunction. The results support a role for REDD1 in diabetes-induced retinal neurodegeneration.

Although diabetic retinopathy (DR) is commonly associated with microvascular dysfunction, significant retinal neurodegeneration occurs early in the course of diabetes (1,2). Altered electroretinograms (ERGs), diminished color vision, and defects in contrast sensitivity (CS) manifest before the

clinical diagnosis of DR can be made by fundus examination (3). A number of previous studies demonstrate that intensive glycemic control is associated with the reduction of pathologies associated with DR and the decline in functional vision (2). Moreover, patients who have not yet developed clinically evident symptoms of retinopathy represent the greatest therapeutic opportunity to improve vision outcomes, because these individuals respond better to intervention (2). Thus, the current study set out to investigate the early molecular mechanisms that mediate retinal neurodegeneration in a model of type 1 diabetes.

The primary cause of diabetes-induced retinal cell death is a combination of hyperglycemia and reduced insulin receptor-mediated signaling (4). In retinal neurons, activation of the insulin receptor drives a prosurvival pathway via phosphatidylinositol 3-kinase (PI3-K)/Akt signaling (5). The retina possesses a constitutively active insulin receptor-signaling system with high basal tyrosine kinase activity that is attenuated by diabetes (6,7). In streptozotocin (STZ)-induced diabetic rats, retinal Akt kinase activity is attenuated as early as 4 weeks after the onset of diabetes (7). Retinal neurons also begin to undergo apoptosis within the same interval (8,9). Similarly, exposure of immortalized retinal neurons (R28 cells) to hyperglycemic conditions reduces insulin-stimulated Akt phosphorylation and cell survival (10). Moreover, subconjunctival insulin administration or systemic glycemic reduction are sufficient to restore activation of the retinal insulin-signaling cascade and promote retinal cell survival in diabetic rats (4). Thus, the molecular mechanisms whereby hyperglycemia contributes to attenuated Akt signaling likely play a role in diabetes-induced retinal neurodegeneration.

¹Department of Cellular and Molecular Physiology, Penn State College of Medicine, Hershey, PA

²Department of Ophthalmology, Penn State College of Medicine, Hershey, PA

Corresponding author: Michael D. Dennis, mdennis@psu.edu.

Received 22 June 2017 and accepted 20 October 2017.

This article contains Supplementary Data online at <http://diabetes.diabetesjournals.org/lookup/suppl/doi:10.2337/db17-0728/-/DC1>.

W.P.M. and C.Y. contributed equally to this work.

© 2017 by the American Diabetes Association. Readers may use this article as long as the work is properly cited, the use is educational and not for profit, and the work is not altered. More information is available at <http://www.diabetesjournals.org/content/license>.

Expression of the stress response Protein Regulated in Development and DNA Damage Response 1 (REDD1; also known as DDIT4/RTP801) in the retina of diabetic mice is enhanced by hyperglycemia, coincident with attenuated activation of the mammalian target of rapamycin (mTOR) in complex 1 (mTORC1) pathway (11). Several studies have identified REDD1 as a potent inhibitor of the mTORC1 pathway, which is activated in response to mitogens (e.g., insulin) and nutrients (e.g., amino acids) and serves to coordinate the effects of such stimuli to regulate diverse cellular processes, including protein synthesis, autophagy, and cell growth (6–8). More recently, our laboratory demonstrated that REDD1 acts to repress the mTORC1 pathway by promoting the association of protein phosphatase 2A with Akt, leading to site-specific dephosphorylation of the kinase, subsequent reduction in Akt-mediated phosphorylation of tuberous sclerosis complex 2, and a fall in the proportion of Rheb in the active guanosine 5'-triphosphate-bound state (12). Direct interaction of Rheb-guanosine 5'-triphosphate, but not Rheb-guanosine 5'-diphosphate, with mTORC1 results in activation of the kinase. REDD1 expression is enhanced in retinal cells in culture exposed to hyperglycemic conditions, Akt phosphorylation is attenuated at the REDD1-sensitive Thr308 site (11). In cell and animal models of Parkinson's disease, enhanced REDD1 expression leads to dephosphorylation of Akt in a manner that causes neuron death (10). Accumulating evidence demonstrates that REDD1 overexpression is sufficient to promote neuronal apoptosis (13,14) and that suppression of the protein has neuroprotective effects on retinal neurons (15,16). However, the effect of diabetes-induced REDD1 expression on retinal cell death has yet to be examined.

In the current study, we assessed the role of diabetes-induced REDD1 in retinal dysfunction. In R28 retinal cells in culture, hyperglycemic conditions enhanced REDD1 protein expression, which was associated with increased cell death. However, neither hyperglycemic conditions nor serum deprivation were sufficient to promote cell death in REDD1-deficient retinal cells. Because REDD1 was necessary for retinal cell death, we evaluated retinal dysfunction in REDD1-deficient STZ-induced diabetic mice. Remarkably, markers of retinal apoptosis and ERG abnormalities were not only absent, but functional vision was also protected in diabetic REDD1-deficient compared with diabetic wild-type mice. Overall, these findings demonstrate a key role for REDD1 in diabetes-induced retinal cell death and vision loss.

RESEARCH DESIGN AND METHODS

Cell Culture

R28 CRISPR (Clustered Regularly Interspaced Short Palindromic Repeats)/Cas9 genome editing to ablate REDD1 expression is described in the Supplementary Data. Cells were maintained on CellBIND culture plates (Corning) with DMEM containing 5 mmol/L glucose, 10% FBS, 1× MEM Non-Essential Amino acids, 1× MEM Vitamin Solution, and 0.14% gentamicin. Where indicated, cells were serum deprived for 24 h in the presence or absence of

100 nmol/L insulin. Cells were also exposed to medium containing 30 mmol/L glucose for 0–24 h. Where indicated, cells were transfected with pCMV5-empty or pCMV5-FOXO1ADA (Addgene Cat # 12149) using Lipofectamine 2000 (Life Technologies).

Animals

Male wild-type and REDD1 knockout C57Bl/6 × 129SvEv mice (16) were given 50 mg/kg STZ for 5 consecutive days to induce diabetes. Control mice were injected with equivalent volumes of sodium citrate buffer. Diabetic phenotype was confirmed by blood glucose concentration >250 mg/dL in freely fed animals. All procedures were approved by the Penn State College of Medicine Institutional Animal Care and Use Committee.

Cell Death ELISA

Cells were lysed in buffer A (see Supplementary Data for buffer compositions). Retinas were homogenized in buffer B using an Eppendorf plastic homogenizer and pellet pestle motor. Relative cell death was assessed using a Cell Death Detection ELISA Kit from Roche (Cat # 11774425001), as previously described (4,17).

AKT Activity Assay

Retinas were homogenized in buffer C. R28 cells were lysed in buffer D. Lysates were spun at 13,000 rpm for 15 min at 4°C. Kinase activity was assessed in supernatants using an Akt Kinase Activity Kit (Abcam, Cat # ab139436).

Western Blot Analysis

Retinas were harvested after 4 weeks of diabetes, flash frozen in liquid nitrogen, and later homogenized in 250 μL extraction buffer, as previously described (18,19). Cell lysates and retinal homogenates were fractionated using Criterion Precast 4–20% gels (Bio-Rad Laboratories, Hercules, CA). Proteins were transferred to polyvinylidene fluoride, reversibly stained to assess protein loading (Pierce), blocked in 5% milk in Tris-buffered saline Tween 20, washed, and incubated overnight at 4°C with the appropriate antibodies found in Supplementary Table 1.

ERG

ERG analysis was used to assess light-induced electrical activity in the eyes of mice after 4 weeks of diabetes. Mice were dark adapted overnight and anesthetized by an intraperitoneal injection of 100 mg ketamine/10 mg xylazine per kg of body weight. All ERG recordings were performed in a dark room under dim red light. Pupils were dilated with 1% tropicamide (Bausch and Lomb). Custom designed ERG recording equipment (Espion E²; Diagnosys, Boston MA) was used. A contact lens recording electrode was placed over the cornea with GenTeal gel (Novartis). A reference electrode was inserted subcutaneously below the eye socket, and a ground electrode was attached to the hind foot. A ganzfeld stimulator (Color-Dome) was lowered over the animal's head and used to generate calibrated flashes of white light ranging from 1×10^{-6} to 100 candela per square meter (cd-s/m²). The

a-wave amplitude was measured from the average pretrial base line to the most negative point of the trace, and the b-wave amplitude was measured from that point to the highest positive point, after subtracting oscillatory potentials (OPs). OPs were isolated using a digital high-pass filter and summed for analysis.

Behavioral Assessment of Vision

The OptoMotry virtual optomotor system (CerebralMechanics, White Plains, NY) was used to evaluate visual function in control and diabetic mice, as previously described (19). Spatial frequency (SF) threshold and CS were assessed using a video camera to monitor elicitation of the optomotor

reflex. CS was assessed at a SF of 0.092 cycles/degree. SF was assessed at 100% contrast. The CS and SF thresholds were identified as the highest values that elicited the reflexive head movement. Both thresholds were averaged over three trials on consecutive days. CS was expressed as an inverse percentage to make data interpretation more intuitive.

Statistical Analysis

Data are expressed as mean ± SEM. Data in Figs. 1–3 and Fig. 6 were analyzed overall with ANOVA, and trend test and pairwise comparisons were conducted with the Tukey test for multiple comparisons. The ERG responses for

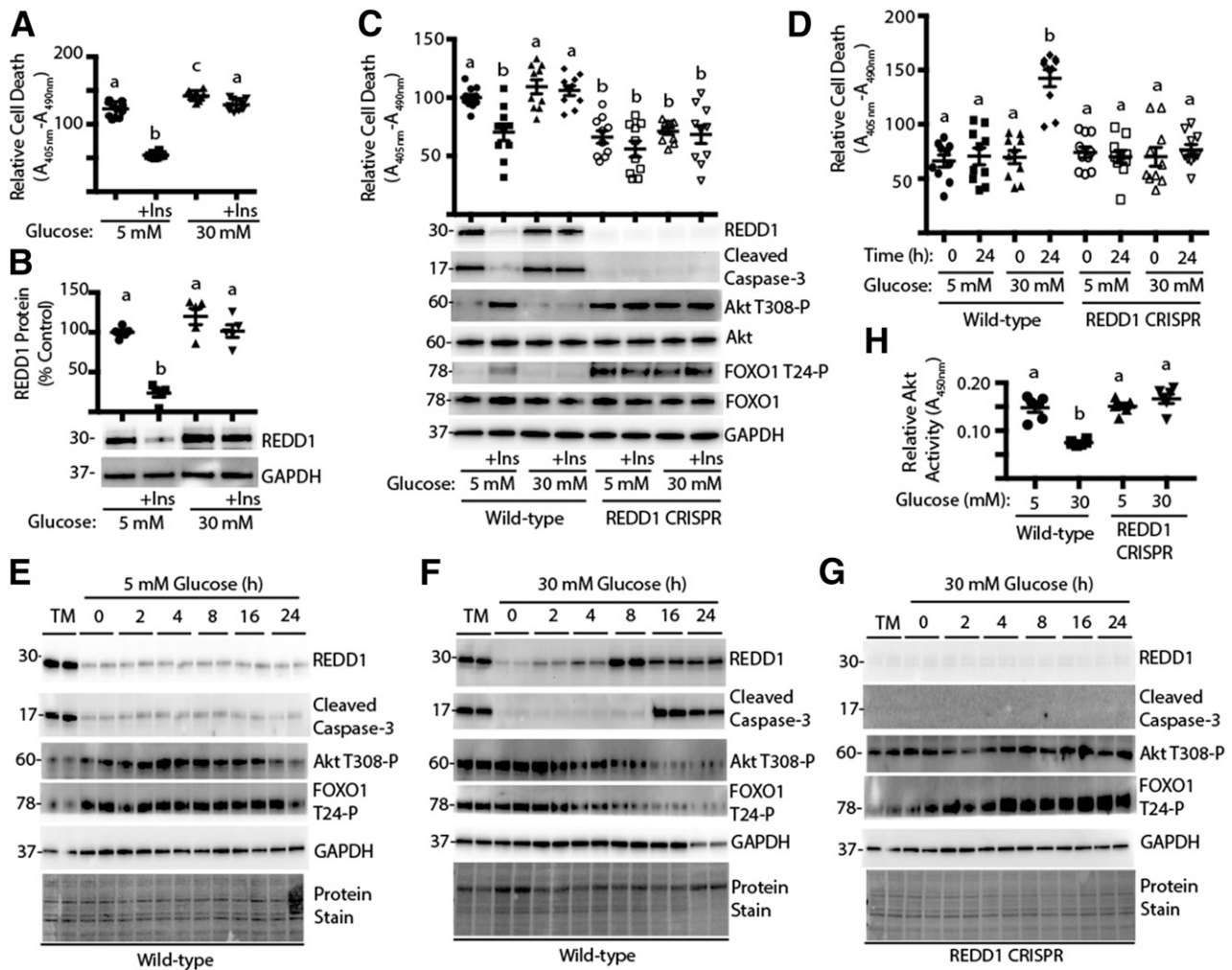


Figure 1—Deletion of REDD1 protects against hyperglycemia-induced retinal cell death. R28 cells were maintained in DMEM containing 5 mmol/L glucose and supplemented with 10% FBS. *A* and *B*: Cells were serum deprived for 24 h in medium containing 5 or 30 mmol/L glucose plus the presence or absence of insulin (+Ins). *C*: Wild-type and REDD1 CRISPR R28 cells were serum deprived for 24 h in medium containing 5 or 30 mmol/L glucose plus the presence or absence of insulin. *D–H*: Wild-type and REDD1 CRISPR R28 cells were exposed to medium containing 10% FBS and 5 or 30 mmol/L glucose for 0–24 h. As a positive control for the induction of REDD1 expression, cells were treated with 2 μg/mL tunicamycin (TM) for 4 h. Relative cell death was assessed by ELISA for cytoplasmic nucleosomes. Expression of REDD1, Akt, FOXO1, GAPDH, caspase-3 cleavage, and phosphorylation of Akt and FOXO1 were assessed by Western blotting. Protein molecular mass in kDa is indicated at the left of the blots. Gel loading was assessed by protein stain. Akt activity in cell lysates was assessed by ELISA using a synthetic peptide substrate. Quantification of Western blots is presented in Supplementary Fig. 2. Values are means ± SE for two independent experiments (*n* = 9–10). Statistical significance is denoted by the presence of different letters above each scatter plot on the graphs. Scatter plots with different letters are statistically different, *P* < 0.05.

diabetic and nondiabetic wild-type or REDD1-deficient mice were compared using repeated-measures ANOVA. In Figs. 4H, 5D, and 5G, a two-sample *t* test compared mean differences in ERG responses between diabetic and nondiabetic mice for wild-type and REDD1-deficient groups. Significance was set at $P < 0.05$ for all analyses.

RESULTS

Hyperglycemic Conditions Promote REDD1 Expression and Cell Death in R28 Cells

To induce hyperglycemic conditions, R28 cells were maintained in medium containing 5 mmol/L glucose, followed by exposure to medium containing 30 mmol/L glucose. In support of previous studies (10), hyperglycemic conditions impaired the effect of insulin to rescue R28 cells from serum deprivation-induced cell death as assessed by the presence of cytoplasmic nucleosomes (Fig. 1A). Insulin treatment also led to a reduction in REDD1 protein expression in serum-deprived R28 cells, whereas hyperglycemic conditions impaired the effect of insulin to do so (Fig. 1B). To determine whether REDD1 played a causal role in cell death, a REDD1-deficient R28 cell line was generated by CRISPR (Supplementary Fig. 1). Cell death induced by serum deprivation was attenuated in REDD1 CRISPR R28 cells compared with wild-type cells when assessed by the presence of cytoplasmic nucleosomes or cleavage of caspase-3, a cysteine protease that becomes active during the late stages of apoptosis (Fig. 1C, and Supplementary Fig. 2A). Increased cleaved caspase-3 expression was not observed in wild-type cells exposed to medium containing 5 mmol/L glucose plus 25 mmol/L mannitol (Supplementary Fig. 3A). Notably, markers of cell death observed in REDD1-deficient cells cultured in the absence of insulin were similar to those observed in wild-type cells cultured in the presence of the hormone (Fig. 1C, and Supplementary Fig. 2A). Moreover, neither insulin nor hyperglycemic conditions had any

effect on the relative level of cell death in REDD1-deficient cells. Similar observations were made in multiple clonal cell lines.

Because serum deprivation (20) and hyperglycemic conditions (11) both promote REDD1 expression, we evaluated the effect of hyperglycemic conditions on REDD1 expression independent of serum deprivation. Compared with cells maintained in medium containing 5 mmol/L glucose, exposure to medium containing 30 mmol/L glucose enhanced the presence of cytoplasmic nucleosomes (Fig. 1D) and caspase-3 cleavage (Fig. 1E and F and Supplementary Fig. 2B) in wild-type R28 cells. In support of the previous report (11), REDD1 protein expression was also enhanced by hyperglycemic conditions. However, in REDD1-deficient cells, exposure to hyperglycemic conditions failed to promote cell death (Fig. 1C and F and Supplementary Fig. 2).

REDD1 Deletion Promotes Akt Activity After Exposure to Hyperglycemic Conditions

Cell death in R28 cells in culture has been previously linked to attenuated activation of PI3-K/Akt signaling (10). Akt-dependent phosphorylation of FOXO transcription factors represses their nuclear localization and thus transcription of proapoptotic target genes (21). Because REDD1 is a key regulator of Akt (12), we investigated phosphorylation of Akt and FOXO1 as well as Akt kinase activity. In serum-deprived cells, phosphorylation of Akt at Thr308 and FOXO1 at Thr24 was enhanced when low-glucose medium was supplemented with insulin (Fig. 1C and Supplementary Fig. 2C and D). By contrast, in serum-deprived REDD1-deficient R28 cells, phosphorylation of Akt and FOXO1 was similar to that observed in wild-type cells cultured in the presence of insulin. Moreover, insulin failed to enhance phosphorylation of Akt or FOXO1 in serum-deprived REDD1-deficient cells. In the absence of hyperglycemic conditions, insulin (Fig. 1C and Supplementary Fig. 2C and D) or the presence of serum in complete cell culture medium

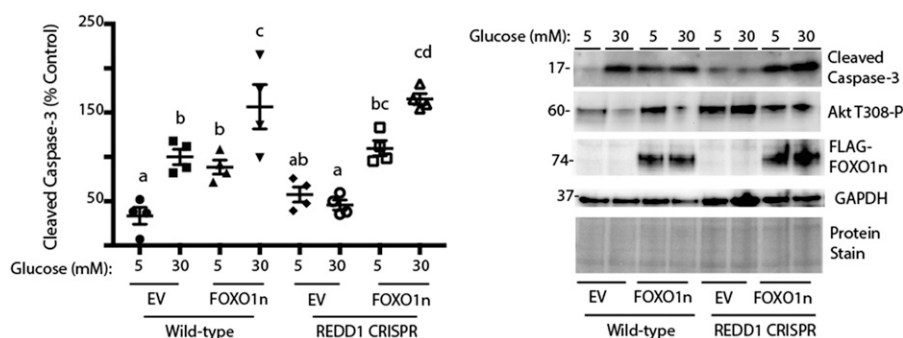


Figure 2—Constitutively nuclear FOXO1 prevents the protective effect of REDD1 deletion. Wild-type and REDD1 CRISPR R28 cells were maintained in DMEM containing 5 mmol/L glucose and supplemented with 10% FBS. Cells were transfected with empty vector (EV) or FOXO1n. Cells were exposed to medium containing 10% FBS and 5 or 30 mmol/L glucose for 24 h. Expression of cleaved caspase-3, phosphorylation of Akt, FLAG-tagged FOXO1n, and GAPDH were assessed by Western blotting. Protein molecular mass in kDa is indicated at the left of the blots. Gel loading was assessed by protein stain. Values are means \pm SE for two independent experiments ($n = 4$). Statistical significance is denoted by the presence of different letters above each scatter plot on the graphs. Scatter plots with different letters are statistically different, $P < 0.05$.

(Fig. 1E and Supplementary Fig. 2E and F) maintained phosphorylation of Akt and FOXO1. However, in the presence of insulin or serum, exposure to medium containing 30 mmol/L glucose was sufficient to repress phosphorylation of Akt and FOXO1 (Figs. 1C and F and 3B), an effect that was absent in REDD1-deficient cells (Fig. 1C and G). Moreover, Akt kinase activity in whole-cell lysates from wild-type cells exposed to hyperglycemic conditions was attenuated, and REDD1 deletion prevented the effect (Fig. 1H). To evaluate the mechanism whereby REDD1 deletion was protective against cell death, we expressed a constitutively nuclear FOXO1 variant (FOXO1n) (22). Compared with wild-type R28 cells, REDD1-deficient cells expressing an empty vector exhibited reduced cleaved caspase-3

expression upon exposure to hyperglycemic conditions; however, the expression of FOXO1n was sufficient to promote cell death in REDD1-deficient cells, such that it was similar to that observed in wild-type cells (Fig. 2).

To evaluate the role of REDD1 in the effect of diabetes on the retina, mice with a germline disruption of REDD1 (16) were administered STZ. After 4 weeks of diabetes, diabetic and nondiabetic REDD1-deficient mice exhibit similar postprandial blood glucose concentrations as those observed in diabetic and nondiabetic wild-type mice (11). In support of our previous report (11), REDD1 protein expression was enhanced in the retina of diabetic wild-type mice compared with nondiabetic controls (Fig. 3A). Alternatively, REDD1 expression was undetectable in the retina of

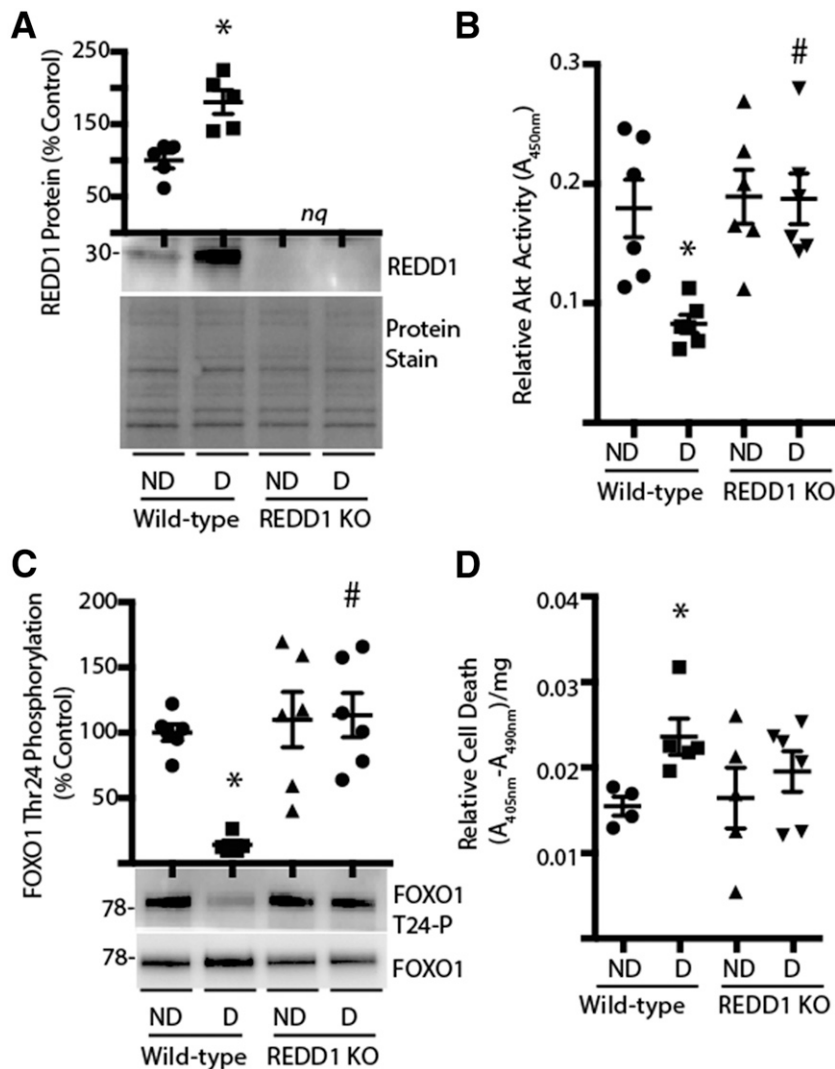


Figure 3—REDD1 ablation prevents diabetes-induced retinal cell death. Retinas were isolated from diabetic (D) and nondiabetic (ND) wild-type and REDD1-knockout (KO) mice 4 weeks after STZ administration. *A*: Expression of REDD1 in retinal lysates was assessed by Western blotting. Gel loading was assessed by protein stain. *B*: Akt activity in retinal lysates was assessed by ELISA by using a synthetic peptide substrate. *C*: FOXO1 phosphorylation was assessed by Western blotting. *D*: Retinal lysates were assayed by ELISA for the presence of nucleosomal fragments in the cytoplasm. Values are means \pm SE for two independent experiments ($n = 5$ –7). * $P < 0.05$ vs. ND and # $P < 0.05$ vs. wild-type. Protein molecular mass in kDa is indicated at the left of blots. nq, no quantification of REDD1 expression was performed on retinal lysates from REDD1-deficient mice.

diabetic and nondiabetic REDD1-knockout mice. A previous study demonstrated that Akt activity is decreased in the retina of rats after 4 weeks of diabetes (7). In support of the previous data, Akt activity (Fig. 3B) and FOXO1 phosphorylation at Thr24 (Fig. 3C) were both attenuated in the retina of diabetic wild-type mice. However, no difference in either of these measures was observed between nondiabetic and diabetic REDD1-deficient mice, and Akt activity and phosphorylation of FOXO1 were both similar to that observed in nondiabetic wild-type mice (Fig. 3B and C).

REDD1 Deletion Prevents Diabetes-Induced Retinal Cell Death

Because REDD1-deficient retinal cells exhibited reduced cell death and Akt activity was maintained in the retina of diabetic REDD1-deficient mice, we next assessed the role of

REDD1 in diabetes-induced cell death in the retina using a cell death ELISA. The presence of cytoplasmic nucleosomes in retinal lysates from diabetic wild-type mice was increased compared with nondiabetic wild-type mice (Fig. 3D). However, no significant difference was found in cytoplasmic nucleosomes in lysates from retinas of diabetic REDD1-deficient mice compared with nondiabetic wild-type mice or nondiabetic REDD1-deficient mice.

Diabetes-Induced Neural Dysfunction Is Absent in REDD1-Deficient Mice

To determine whether REDD1 ablation was sufficient to prevent diabetes-induced retinal dysfunction, we evaluated full-field stimulus-evoked ERGs in eyes of diabetic and nondiabetic REDD1-deficient mice. Scotopic ERGs were recorded at increasing stimulus intensities and then analyzed for a- and

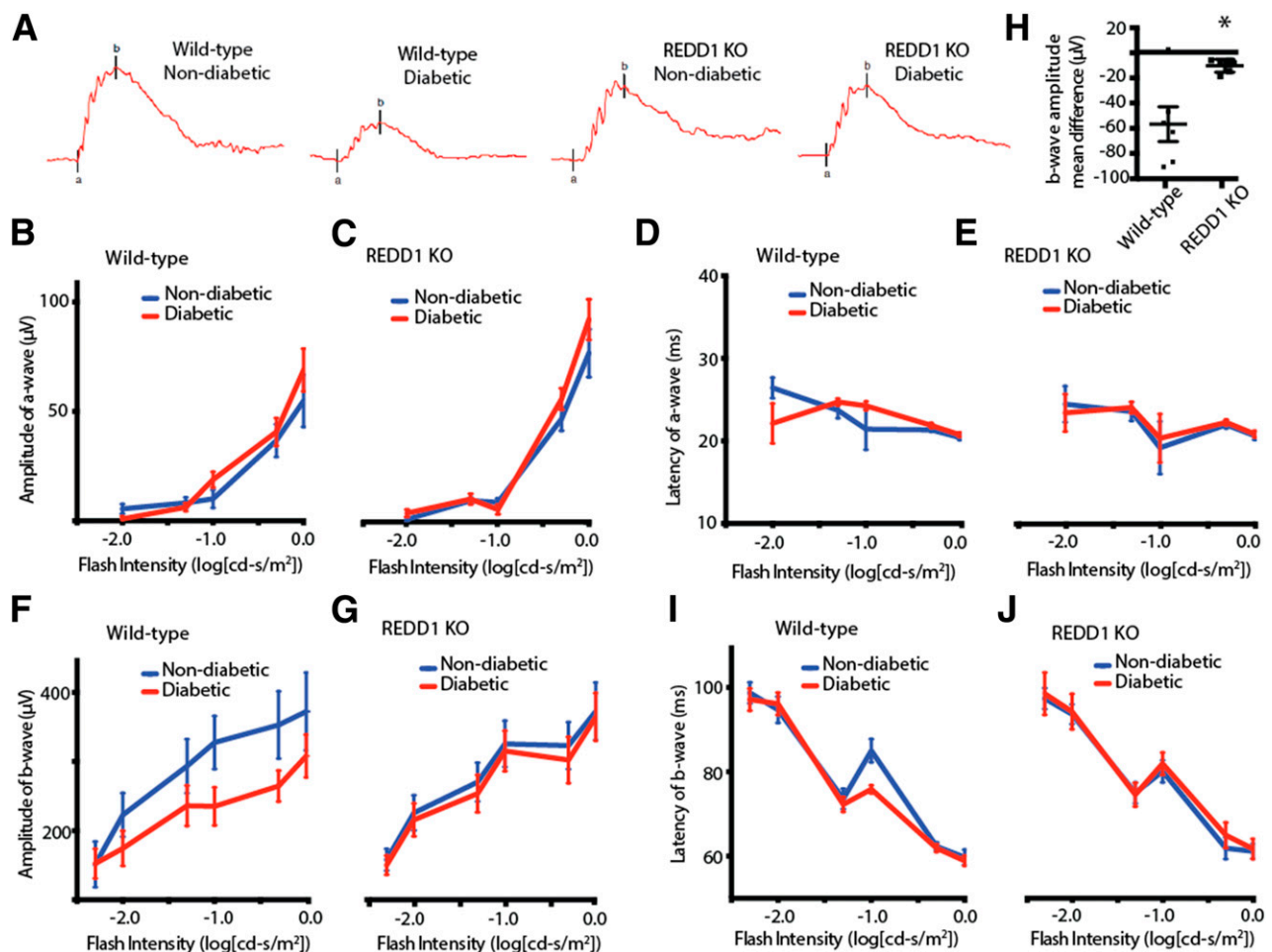


Figure 4—REDD1 ablation reduces the attenuation of b-wave amplitudes in response to diabetes. At 4 weeks after STZ administration, scotopic ERG responses were recorded from the eyes of diabetic and nondiabetic wild-type and REDD1-knockout (KO) mice at increasing stimulus intensities. *A*: Representative ERG response elicited from -1.0 cd-s/m² log flash intensity. ERG a-wave amplitudes are plotted against the stimulus flash intensity for nondiabetic and diabetic wild-type (*B*) and REDD1-deficient mice (*C*). The corresponding implicit times are shown for a-waves of nondiabetic and diabetic wild-type (*D*) and REDD1-deficient mice (*E*). ERG b-wave amplitudes are plotted against the flash intensity of stimulus luminance for nondiabetic and diabetic wild-type (*F*) and REDD1-deficient mice (*G*). *H*: Mean difference in b-wave amplitudes of nondiabetic and diabetic mice across flash intensities. The corresponding implicit times are shown for b-waves of nondiabetic and diabetic wild-type (*I*) and REDD1-deficient mice (*J*). Values are means \pm SE for two independent experiments ($n = 8$). * $P < 0.05$ vs. wild-type. Graphs in *C*, *E*, *G*, and *J* share the y-axis with *B*, *D*, *F*, and *I*, respectively.

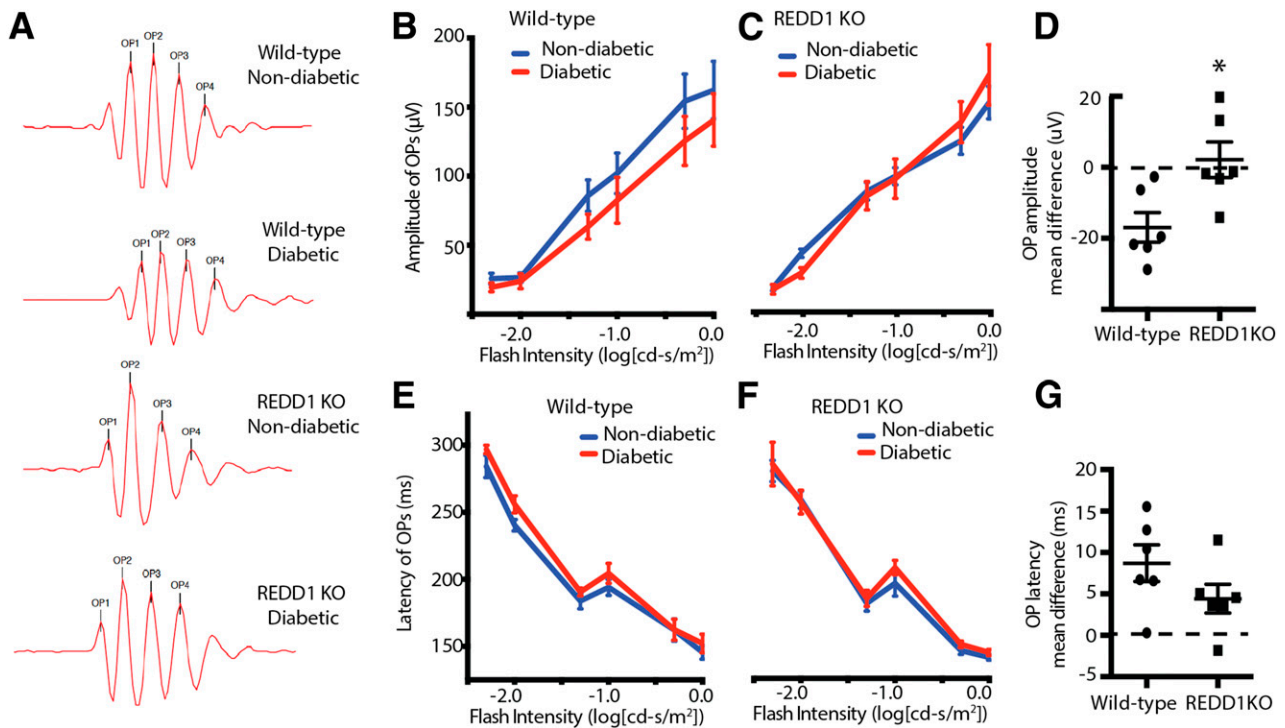


Figure 5—REDD1 ablation prevents attenuated OP amplitudes in response to diabetes. At 4 weeks after STZ administration, scotopic ERG responses were recorded from diabetic and nondiabetic wild-type and REDD1-knockout (KO) mice after overnight dark adaptation. A high-pass filter was used to extract OPs from raw ERG recordings. **A**: Representative OPs elicited from -1.0 cd-s/m^2 log flash intensity. Summed OP amplitudes are plotted against the stimulus flash intensity for nondiabetic and diabetic wild-type (**B**) and REDD1-KO mice (**C**). **D**: Comparison of the mean difference in summed OP amplitudes for wild-type and REDD1-KO mice. The corresponding implicit times of nondiabetic and diabetic wild-type (**E**) and REDD1-deficient mice (**F**) are shown. **G**: Comparison of the mean difference in summed OP implicit times for wild-type and REDD1-KO mice between nondiabetic and diabetic mice. Values are means \pm SE for two independent experiments ($n = 8$). * $P < 0.05$ vs. wild-type. Graphs in **C** and **F** share the y-axis with **B** and **E**, respectively.

b-wave amplitudes and implicit times (Fig. 4A). After 4 weeks of diabetes, a-wave amplitudes and implicit times were not different in wild-type or REDD1-deficient mice (Fig. 4B and E). In contrast, b-wave amplitudes were reduced in diabetic wild-type mice compared with nondiabetic controls (Fig. 4F). Moreover, diabetic REDD1-deficient mice also exhibited a small but significant reduction in b-wave amplitudes compared with nondiabetic REDD1-deficient mice (Fig. 4G). Specifically, the deficit in the mean b-wave amplitude between diabetic and nondiabetic REDD1-deficient mice was $\sim 20\%$ of that observed in wild-type mice (Fig. 4H). The implicit time of maximal b-wave response was not altered by diabetes in wild-type or REDD1-deficient mice (Fig. 4I and J).

Raw ERG waves were processed through a digital high-pass filter to isolate OPs (Fig. 5A). Whereas OP amplitudes were attenuated in diabetic wild-type mice (Fig. 5B), diabetic and nondiabetic REDD1-deficient mice exhibited similar OP amplitudes (Fig. 5C). Thus, wild-type mice exhibited a greater deficit in mean OP amplitude between diabetic and nondiabetic mice compared with REDD1-deficient mice (Fig. 5D). The implicit time of OPs of diabetic wild-type mice was significantly increased compared with nondiabetic controls (Fig. 5E). Alternatively, the implicit time of OPs of diabetic and nondiabetic REDD1-deficient mice was not

different (Fig. 5F). However, the mean difference in OP latency for REDD1-deficient mice was not significantly different from the mean difference in OP latency of wild-type mice (Fig. 5G).

REDD1 Ablation Protects Mice From the Early Effects of Diabetes on Functional Vision

The effect of diabetes on functional vision was directly assessed in REDD1-deficient mice by measurement of the optomotor response. Diabetic wild-type mice exhibited a deficit in SF 4 weeks after STZ administration, but REDD1-deficient mice failed to do so (Fig. 6A). Similarly, CS was attenuated in diabetic wild-type mice compared with nondiabetic wild-type mice; however, the CS results of diabetic and nondiabetic REDD1-deficient mice were similar to those of nondiabetic wild-type mice (Fig. 6B). Importantly, the CS of diabetic REDD1-deficient mice was significantly elevated compared with diabetic wild-type controls. A similar protective effect of REDD1 ablation was observed in SF and CS after 8 weeks of diabetes, because both values were attenuated in diabetic wild-type mice compared with nondiabetic controls yet were not different in diabetic and nondiabetic REDD1-deficient mice (Fig. 6C and D). However, SF at 8 weeks was attenuated in nondiabetic REDD1-deficient mice compared with wild-type controls.

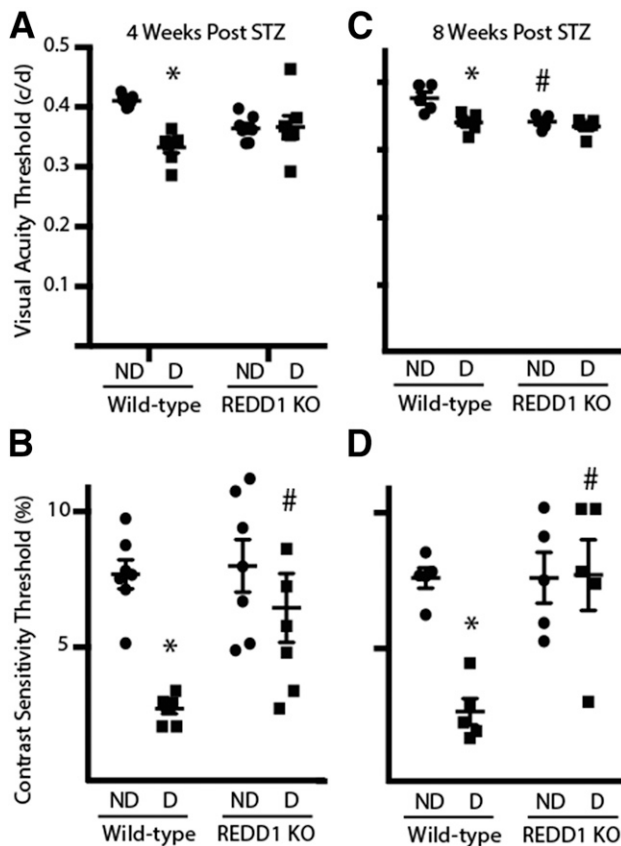


Figure 6—Diabetes-induced visual dysfunction is absent in REDD1-deficient mice. Visual function was assessed by virtual optomotor testing after 4 (A and B) and 8 weeks (C and D) of diabetes. SF (A and C) and CS (B and D) thresholds were obtained in nondiabetic (ND) and diabetic (D) wild-type and REDD1-knockout (KO) mice. The CS threshold is expressed as the reciprocal value of the CS score. Values are means \pm SE for two independent experiments ($n = 5-7$). * $P < 0.05$ vs. control and # $P < 0.05$ vs. wild-type. Graphs in C and D share the y-axis labels with A and B, respectively. c/d, cycles/degree.

DISCUSSION

The current study investigated the role of REDD1 protein expression in diabetes-induced retinal dysfunction. Overall, the findings support a model whereby diabetes promotes REDD1 expression in a manner that contributes to retinal cell death and visual dysfunction. In R28 retinal cells in culture, hyperglycemic conditions enhanced REDD1 protein expression and apoptosis. Alternatively, when REDD1 expression was ablated by CRISPR, neither serum deprivation nor hyperglycemic conditions were sufficient to promote cell death. Because REDD1 expression was necessary for the effects of hyperglycemic conditions and serum deprivation on retinal cell death in culture, we evaluated apoptosis in the retina of diabetic mice. In accordance with previous reports of diabetes-induced neuroretinal apoptosis (8), diabetic mice exhibited an increase in cell death 4 weeks after STZ administration. However, the effect of diabetes was absent in retinas from REDD1-deficient mice.

In a previous study, we provided evidence that diabetes-induced hyperglycemia enhanced REDD1 expression, attenuated Akt/mTORC1 signaling, and promoted translation of vascular endothelial growth factor (VEGF) mRNA (11). VEGF levels are elevated in the vitreous fluid of patients with DR (23), and the cytokine is considered a major molecular mechanism in retinal vascular complications (24). Therapeutic blockade of VEGF has seen widespread use in the treatment of diabetic macular edema and proliferative DR. However, systemic VEGF neutralization is associated with significant neural cell death and decline of retinal function as assessed by ERG (25). Importantly, REDD1 deletion does not attenuate basal VEGF expression but rather prevents the increase in its expression in response to hyperglycemic conditions (11). The current study extends our previous work by demonstrating that REDD1 also contributes to retinal apoptosis and visual dysfunction in a model of type 1 diabetes. However, reduced neuroretinal function observed in STZ-induced REDD1-deficient mice is unlikely to be due to normalized VEGF expression. Rather, the current study supports a mechanism whereby REDD1 deficiency maintains Akt activity and prevents FOXO1-dependent neuronal apoptosis.

In retinal neurons, activation of Akt plays a key role in survival (5). Akt activity is regulated by the coordinate phosphorylation and dephosphorylation of multiple Ser/Thr residues. In response to insulin and growth factors, the activation loop of Akt is phosphorylated by PDK1 at Thr308 (26), and the hydrophobic motif is subsequently phosphorylated by mTORC2 at Ser473 (27). Hyperglycemic conditions attenuate insulin-stimulated phosphorylation of Akt in R28 cells in culture through a mechanism downstream of insulin receptor substrate 1 (IRS-1) and PI3-K (10). Unlike Akt, insulin-stimulated phosphorylation of IRS-1 and coimmunoprecipitation of IRS-1 with the p85 subunit of PI3-K are not attenuated in R28 cells after exposure to hyperglycemic conditions (10). One possible mechanism that could account for the repressive effect of hyperglycemic conditions on Akt activation in the absence of a reduction in IRS-1/PI3-K activity is enhanced REDD1 expression.

REDD1 represses Akt activity through recruitment of protein phosphatase 2A and dephosphorylation of the kinase on Thr308 (12). Enhanced REDD1 expression is associated with attenuated phosphorylation of Akt substrates, including tuberous sclerosis complex 2, glycogen synthase kinase 3, and FOXO1/3 (12). When R28 retinal cells were exposed to medium containing high glucose concentrations, enhanced REDD1 protein expression mediated a reduction in Akt phosphorylation at Thr-308 and attenuated phosphorylation of FOXO1. Akt-mediated phosphorylation of FOXO1 promotes association of the protein with 14-3-3, translocation from the nucleus and thus transcriptional inactivation (28). In the current study, expression of a FOXO1 variant that resists phosphorylation-dependent exclusion from the nucleus was sufficient to prevent the protective effects of REDD1 deletion on caspase-3 cleavage

in response to hyperglycemic conditions in R28 cells. This observation supports the previous report that FOXO1 DNA binding and nuclear translocation is enhanced in the retinal microvasculature of diabetic rodents and that FOXO1 knockdown by small interfering (si)RNA reduces microvascular cell apoptosis in diabetic retinas and in retinal endothelial cells exposed to hyperglycemic conditions (29).

To evaluate the functional consequences of REDD1 deletion on diabetes-induced retinal dysfunction, we performed ERG analysis and assessed functional vision using a behavioral optokinetic apparatus. STZ induced ERG waveform abnormalities in wild-type mice; however, these abnormalities were absent or greatly diminished in REDD1-deficient mice. Although measures of functional vision were reduced in diabetic wild-type mice compared with nondiabetic controls, a similar deficit could not be observed in diabetic REDD1-deficient mice compared with nondiabetic REDD1-knockout mice or nondiabetic wild-type mice. One caveat to this observation is that SF at 8 weeks was attenuated in nondiabetic REDD1-deficient mice compared with wild-type controls. Thus, these observations fail to indicate a protective effect of REDD1 deletion on SF but rather the absence of an additive diabetes-induced deficiency. The protective effects of REDD1 deletion were principally observed in CS, which is associated with inner retinal information processing, compared with the outer retina and photoreceptors. Diabetes-induced hyperglycemia enhances REDD1 protein expression in the retina of diabetic wild-type mice compared with nondiabetic controls (11). Unfortunately, presently available REDD1 antibodies are not sufficient to evaluate localization of REDD1 protein expression by immunohistochemistry. However, *in situ* hybridization has been used to demonstrate that REDD1 mRNA expression is enhanced in the inner retina of a mouse model of retinopathy of prematurity and necessary for hypoxia-induced retinal apoptosis (16). Whereas the retinas of normoxic mice display only a weak background hybridization signal in all retinal layers, retinas from hypoxic mice exhibit a significantly elevated signal with maximum concentrations in the outer portion of the inner nuclear layer. Overall, the effects of REDD1 deletion on diabetes-induced ERG abnormalities and defects in CS are consistent with a model wherein diabetes-induced REDD1 promotes inner retinal dysfunction.

Alterations in the electrical response of the neural retina to flashes of light are one of the earliest symptoms of DR in patients (30). Alterations in the OP of the b-wave are the most cited and studied ERG abnormality associated with DR (31), because OP abnormalities have been shown to predict the onset and progression of DR (32). These high-frequency wavelets occur during the rising phase of the b-wave and arise from the inner retina (33). In diabetic rats, OP abnormalities are observed as early as 2 weeks after STZ is administered (34). In the current study, we observed a reduction in the mean OP amplitude and an extended OP latency in diabetic wild-type mice 4 weeks after STZ was administered; however, neither of these measures was altered by diabetes in REDD1-deficient mice. Diabetes also

reduced b-wave amplitudes in both mouse strains, although the magnitude of reduction in wild-type mice was fivefold more than that observed in REDD1-deficient mice. This finding supports previous reports that b-wave amplitudes are attenuated in rodent models of diabetes after only a few weeks of hyperglycemia (35).

Apoptosis of retinal neurons is accelerated by diabetes, and the onset of the increase in cell death is early in the nonproliferative stages of disease progression. Accordingly, therapeutic approaches that prevent neuroretinal dysfunction are of particular interest. One such approach would be intravitreal injection of the siRNA PF-04523655 (36), which reduces REDD1 mRNA expression in the retina of diabetic rodents (37) and improves visual acuity in patients with diabetic macular edema (38). Notably, improved vision in patients treated with PF-04523655 occurs in the absence of altered anatomical features or fluorescein leakage, suggesting a mechanism independent of reduced vascular permeability (38). The findings here provide new insight into the mechanism whereby REDD1-targeted siRNAs improve vision outcomes in patients with diabetic macular edema. In the retina of STZ-induced diabetic mice, REDD1 protein expression was increased concomitant with retinal cell death and impaired visual function. However, REDD1 deletion was sufficient to prevent diabetes-induced retinal cell death and visual dysfunction in a rodent model of type 1 diabetes. Thus, the findings here support a neuroprotective mechanism for REDD1-targeted therapeutics in the prevention of diabetes-induced visual dysfunction.

Acknowledgments. The authors gratefully acknowledge Drs. Leonard Jefferson and Scot Kimball (Penn State College of Medicine) for critically evaluating the manuscript. The authors thank Dr. Elena Feinstein (Quark Pharmaceuticals) for permission to use the REDD1 knockout mice, Dr. Gail Seigel (Ross Eye Institute, SUNY, Buffalo, NY) for permission to use the R28 retinal cell line, and Allyson Torro (Penn State College of Medicine) for technical assistance in the performance of the studies described herein.

Funding. This work was supported by the American Diabetes Association Pathway to Stop Diabetes Grant 1-14-INI-04, National Eye Institute grant EY023612, and the Penn State Eye Center Frontiers in Eye and Vision Research Award (to M.D.D.).

Duality of Interest. No potential conflicts of interest relevant to this article were reported.

Author Contributions. W.P.M. researched data and wrote the manuscript. C.Y. and M.L.M. executed experiments. J.A.M. and W.D. designed and validated the R28 CRISPR knockout R28 cell line. A.J.B. designed experiments and reviewed and edited the manuscript. M.D.D. designed experiments, researched the data, and wrote, reviewed, and edited the manuscript. M.D.D. is the guarantor of this work and, as such, had full access to all the data in the study and takes responsibility for the integrity of the data and the accuracy of analysis.

Prior Presentation. Parts of this study were presented in abstract form at the 76th Scientific Sessions of the American Diabetes Association, New Orleans, LA, 10–14 June 2016.

References

- Ghirlanda G, Di Leo MA, Caputo S, Cercone S, Greco AV. From functional to microvascular abnormalities in early diabetic retinopathy. *Diabetes Metab Rev* 1997; 13:15–35

2. Han Y, Barse MA Jr, Schneck ME, Barez S, Jacobsen CH, Adams AJ. Multifocal electroretinogram delays predict sites of subsequent diabetic retinopathy. *Invest Ophthalmol Vis Sci* 2004;45:948–954
3. Gardner TW, Davila JR. The neurovascular unit and the pathophysiologic basis of diabetic retinopathy. *Graefes Arch Clin Exp Ophthalmol* 2017;255:1–6
4. Fort PE, Losiewicz MK, Reiter CE, et al. Differential roles of hyperglycemia and hypoinsulinemia in diabetes induced retinal cell death: evidence for retinal insulin resistance. *PLoS One* 2011;6:e26498
5. Barber AJ, Nakamura M, Wolpert EB, et al. Insulin rescues retinal neurons from apoptosis by a phosphatidylinositol 3-kinase/Akt-mediated mechanism that reduces the activation of caspase-3. *J Biol Chem* 2001;276:32814–32821
6. Reiter CE, Sandirasegarane L, Wolpert EB, et al. Characterization of insulin signaling in rat retina in vivo and ex vivo. *Am J Physiol Endocrinol Metab* 2003;285:E763–E774
7. Reiter CE, Wu X, Sandirasegarane L, et al. Diabetes reduces basal retinal insulin receptor signaling: reversal with systemic and local insulin. *Diabetes* 2006;55:1148–1156
8. Barber AJ, Lieth E, Khin SA, Antonetti DA, Buchanan AG, Gardner TW. Neural apoptosis in the retina during experimental and human diabetes. Early onset and effect of insulin. *J Clin Invest* 1998;102:783–791
9. Barber AJ, Antonetti DA, Kern TS, et al. The *Ins2Akita* mouse as a model of early retinal complications in diabetes. *Invest Ophthalmol Vis Sci* 2005;46:2210–2218
10. Nakamura M, Barber AJ, Antonetti DA, et al. Excessive hexosamines block the neuroprotective effect of insulin and induce apoptosis in retinal neurons. *J Biol Chem* 2001;276:43748–43755
11. Dennis MD, Kimball SR, Fort PE, Jefferson LS. Regulated in development and DNA damage 1 is necessary for hyperglycemia-induced vascular endothelial growth factor expression in the retina of diabetic rodents. *J Biol Chem* 2015;290:3865–3874
12. Dennis MD, Coleman CS, Berg A, Jefferson LS, Kimball SR. REDD1 enhances protein phosphatase 2A-mediated dephosphorylation of Akt to repress mTORC1 signaling. *Sci Signal* 2014;7:ra68
13. Malagelada C, Ryu EJ, Biswas SC, Jackson-Lewis V, Greene LA. RTP801 is elevated in Parkinson brain substantia nigral neurons and mediates death in cellular models of Parkinson's disease by a mechanism involving mammalian target of rapamycin inactivation. *J Neurosci* 2006;26:9996–10005
14. Shoshani T, Faerman A, Mett I, et al. Identification of a novel hypoxia-inducible factor 1-responsive gene, RTP801, involved in apoptosis. *Mol Cell Biol* 2002;22:2283–2293
15. Morgan-Warren PJ, O'Neill J, de Cogan F, et al. siRNA-mediated knockdown of the mTOR inhibitor RTP801 promotes retinal ganglion cell survival and axon elongation by direct and indirect mechanisms. *Invest Ophthalmol Vis Sci* 2016;57:429–443
16. Brafman A, Mett I, Shafir M, et al. Inhibition of oxygen-induced retinopathy in RTP801-deficient mice. *Invest Ophthalmol Vis Sci* 2004;45:3796–3805
17. Abcouwer SF, Lin CM, Wolpert EB, et al. Effects of ischemic preconditioning and bevacizumab on apoptosis and vascular permeability following retinal ischemia-reperfusion injury. *Invest Ophthalmol Vis Sci* 2010;51:5920–5933
18. Gastinger MJ, Singh RS, Barber AJ. Loss of cholinergic and dopaminergic amacrine cells in streptozotocin-diabetic rat and *Ins2Akita*-diabetic mouse retinas. *Invest Ophthalmol Vis Sci* 2006;47:3143–3150
19. Miller WP, Mihailescu ML, Yang C, et al. The translational repressor 4E-BP1 contributes to diabetes-induced visual dysfunction. *Invest Ophthalmol Vis Sci* 2016;57:1327–1337
20. Dennis MD, McGhee NK, Jefferson LS, Kimball SR. Regulated in DNA damage and development 1 (REDD1) promotes cell survival during serum deprivation by sustaining repression of signaling through the mechanistic target of rapamycin in complex 1 (mTORC1). *Cell Signal* 2013;25:2709–2716
21. Gilley J, Coffey PJ, Ham J. FOXO transcription factors directly activate bim gene expression and promote apoptosis in sympathetic neurons. *J Cell Biol* 2003;162:613–622
22. Kitamura YI, Kitamura T, Kruse JP, et al. FoxO1 protects against pancreatic beta cell failure through NeuroD and MafA induction. *Cell Metab* 2005;2:153–163
23. Aiello LP, Avery RL, Arrigg PG, et al. Vascular endothelial growth factor in ocular fluid of patients with diabetic retinopathy and other retinal disorders. *N Engl J Med* 1994;331:1480–1487
24. Miller JW, Adamis AP, Shima DT, et al. Vascular endothelial growth factor/vascular permeability factor is temporally and spatially correlated with ocular angiogenesis in a primate model. *Am J Pathol* 1994;145:574–584
25. Saint-Geniez M, Maharaj AS, Walshe TE, et al. Endogenous VEGF is required for visual function: evidence for a survival role on Müller cells and photoreceptors. *PLoS One* 2008;3:e3554
26. Alessi DR, James SR, Downes CP, et al. Characterization of a 3-phosphoinositide-dependent protein kinase which phosphorylates and activates protein kinase Balpha. *Curr Biol* 1997;7:261–269
27. Sarbassov DD, Guertin DA, Ali SM, Sabatini DM. Phosphorylation and regulation of Akt/PKB by the rictor-mTOR complex. *Science* 2005;307:1098–1101
28. Xie Q, Chen J, Yuan Z. Post-translational regulation of FOXO. *Acta Biochim Biophys Sin (Shanghai)* 2012;44:897–901
29. Behl Y, Krothapalli P, Desta T, Roy S, Graves DT. FOXO1 plays an important role in enhanced microvascular cell apoptosis and microvascular cell loss in type 1 and type 2 diabetic rats. *Diabetes* 2009;58:917–925
30. Tzekov R, Arden GB. The electroretinogram in diabetic retinopathy. *Surv Ophthalmol* 1999;44:53–60
31. Juen S, Kieselbach GF. Electrophysiological changes in juvenile diabetics without retinopathy. *Arch Ophthalmol* 1990;108:372–375
32. Bresnick GH, Korth K, Groo A, Palta M. Electroretinographic oscillatory potentials predict progression of diabetic retinopathy. Preliminary report. *Arch Ophthalmol* 1984;102:1307–1311
33. Ogden TE. The oscillatory waves of the primate electroretinogram. *Vision Res* 1973;13:1059–1074
34. Sakai H, Tani Y, Shirasawa E, Shirao Y, Kawasaki K. Development of electroretinographic alterations in streptozotocin-induced diabetes in rats. *Ophthalmic Res* 1995;27:57–63
35. Li Q, Zemel E, Miller B, Perlman I. Early retinal damage in experimental diabetes: electroretinographical and morphological observations. *Exp Eye Res* 2002;74:615–625
36. Nguyen QD, Schachar RA, Nduaka CI, et al.; MONET Clinical Study Group. Evaluation of the siRNA PF-04523655 versus ranibizumab for the treatment of neovascular age-related macular degeneration (MONET Study). *Ophthalmology* 2012;119:1867–1873
37. Rittenhouse KD, Johnson TR, Vicini P, et al. RTP801 gene expression is differentially upregulated in retinopathy and is silenced by PF-04523655, a 19-Mer siRNA directed against RTP801. *Invest Ophthalmol Vis Sci* 2014;55:1232–1240
38. Nguyen QD, Schachar RA, Nduaka CI, et al.; DEGAS Clinical Study Group. Dose-ranging evaluation of intravitreal siRNA PF-04523655 for diabetic macular edema (the DEGAS study). *Invest Ophthalmol Vis Sci* 2012;53:7666–7674